Current Pharmacology Reports (2020) 6:121–130
https://doi.org/10.1007/s40495-020-00220-x

NANODRUGS (ATY LAU, SECTION EDITOR)

The Cytotoxic Effect of *Annona muricata*-Loaded PHB-Coated Magnetic Nanoparticles on Cancer Cell Lines and Molecular Docking Analyses

Rana Köksal[1] · Serap Yalcin[2]

Published online: 13 June 2020

Abstract
In this study, we designed PHB-coated iron oxide–based nanoparticle for the delivery of *Annona muricata* to breast cancer cells and analyzed its therapeutic efficacy in vitro. The structural properties, functional groups, size distribution, and magnetic properties of the synthesized PHB-coated magnetic nanoparticles (MNPs) were characterized in our previous study. The current study visualized protein–ligand interactions by the use of molecular docking. The plant extract was loaded onto PHB-MNPs in different concentrations and the release efficiencies at different pHs were studied under in vitro conditions. The most efficient loading concentration was found about 55% in pH 7.4. The extract-loaded MNPs were stable up to 3 months in neutral pH for mimicking physiological conditions. The release studies were performed with acetate buffer (pH 4.2) that mimics endosomal pH. The plant extract-loaded PHB-MNPs were about 2.5–3-fold more cytotoxic as compared with free plant extract on HeLa and MDA-MB-231 in vitro, respectively. The cytotoxicity results also confirm that anti-apoptotic proteins have the best docking score for isoquercetin–PHB-MNPs, roseoside–PHB-MNPs, and anonaine–PHB-MNPs with molecular docking analyses. Based on the results obtained, this system can be used effectively in cancer treatment.

Keywords *Annona muricata* · PHB-MNPs · Extract-loaded PHB-MNPs · In vitro cytotoxicity · Cancer cells · Molecular docking

Introduction

In the last century, nanotechnology has attracted attention due to its many unique physical and chemical features, and wide applications especially in medicine and biotechnology research [1]. Iron oxide nanoparticles have been used as the most potential nanoparticle systems for cancer treatment, owing to their super-paramagnetic and surface modification properties [2]. Studies have suggested that iron oxide nanoparticles can be an excellent route for targeted drug delivery in cancer treatment [3, 4].

Different organic and inorganic coatings play an important role in the nano-based drug carrier systems capacity [5]. Polymeric magnetic nanoparticles have been used in targeted drug delivery extensively for various active compounds including drug, siRNA, miRNA, extract, and so on. Polyhydroxybutyrate (PHB) are biodegradable polymers used in nanoparticles due to their biocompatibility and continuous-release properties [6–9]. Therefore, new drug discovery aims to extinguish the toxicity of chemotherapeutic agents, developing more effective drugs to improve treatments, eliminating poor prognosis, and protecting healthy cells [10].

Nowadays, *Annona muricata* L., a plant of the family Annonaceae, has been widely investigated due to its therapeutic potential [11–14]. *A. muricata* have various phytochemicals including alkaloids (ALKs), megastigmane (MGs), flavonoid tri glycosides (FTGs), phenolics (PLs), cyclopeptides (CPs), and volatile oils. The major component of *A. muricata* is acetogenins (AGEs), which have been isolated from leaves, bark, seeds, roots, and fruits of the plant [15]. Acetogenins lead the cells to apoptosis by disrupting mitochondrial membrane potential in cancer

This article is part of the Topical Collection on *Nanodrugs*

✉ Serap Yalcin
serapyalcin1982@gmail.com; syalcin@ahievran.edu.tr

[1] Department of Advanced Technology, Kırsehir Ahi Evran University, Kırsehir, Turkey

[2] Department of Molecular Biology and Genetics, Kırsehir Ahi Evran University, Kırsehir, Turkey

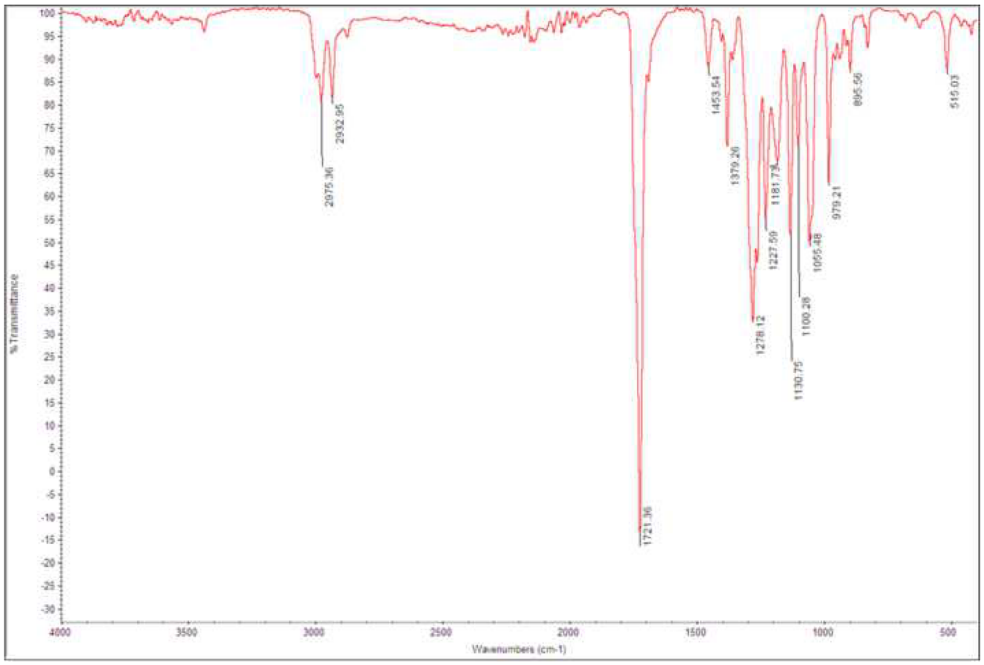

Fig. 1 FTIR analyses of pure PHB

cells [14, 16, 17]. It has been known that AGEs have potential for anticancer activity, thus the plant extract was loaded by using polymer-coated magnetic nanoparticles as a carrier for better anticancer activity in this study. Furthermore, nanoparticles have been prepared in order to enhance stability, internalization, efficacy, and targeted and therapeutic dose of *A. muricata*. The loading of the plant extract into nano-based systems has been widely studied in the literature [14, 18, 19].

In this study, we have demonstrated the cytotoxic effect of plant extract–loaded PHB-coated magnetic nanoparticle and compare with free extract and free nanoparticle on HeLa and MDA-MB-231 cell lines. The physicochemical properties of the extract-loaded

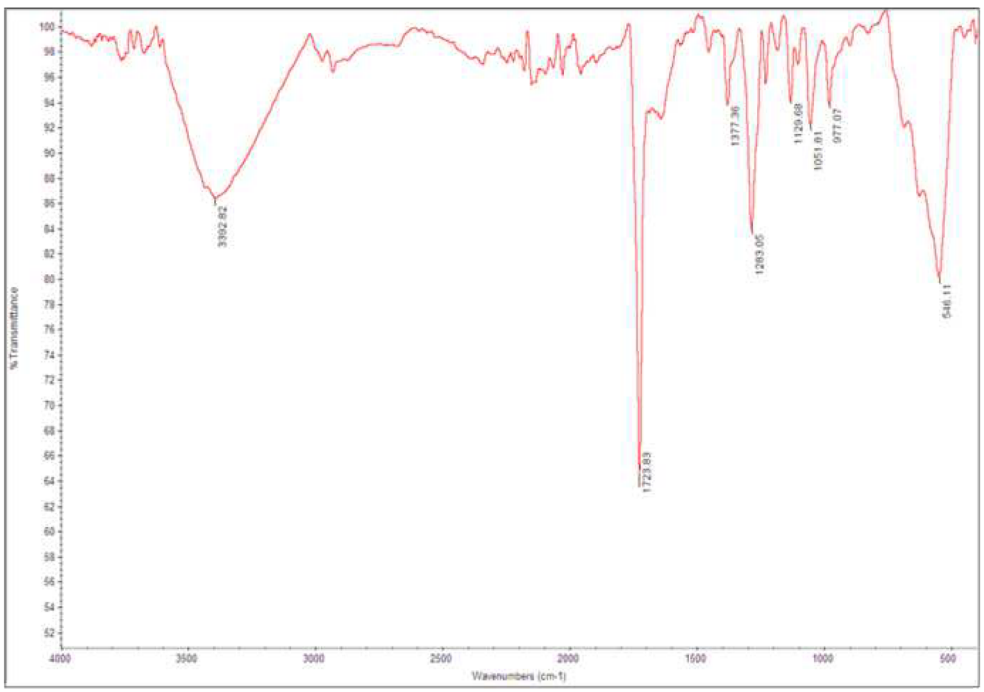

Fig. 2 FTIR analyses of PHB-MNPs

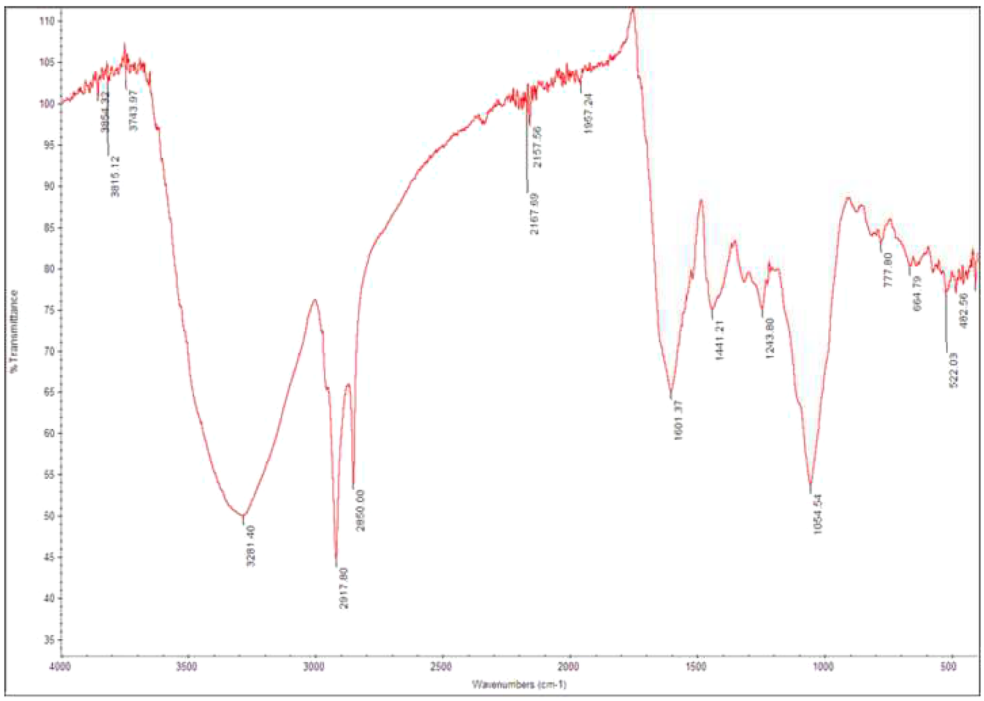

Fig. 3 FT-IR analyses of pure *Annona muricata* extract

nanoparticles were characterized, and their in vitro release, stability profiles, and cytotoxicity activity were analyzed on cancer cells. Furthermore, to evaluate the potential of these drug systems for the treatment of cancer, we tested molecular docking analyses against anti-apoptotic proteins.

Materials and Methods

Iron (II) chloride tetrahydride ($FeCl_2{\cdot}4H_2O$) and iron (III) chloride hexahydrate ($FeCl_3{\cdot}6H_2O$) were obtained from Merck (Germany); polyhydroxybutyrate (PHB) and ammonium hydroxide (NH_4OH), RPMI-1640 medium, fetal bovine

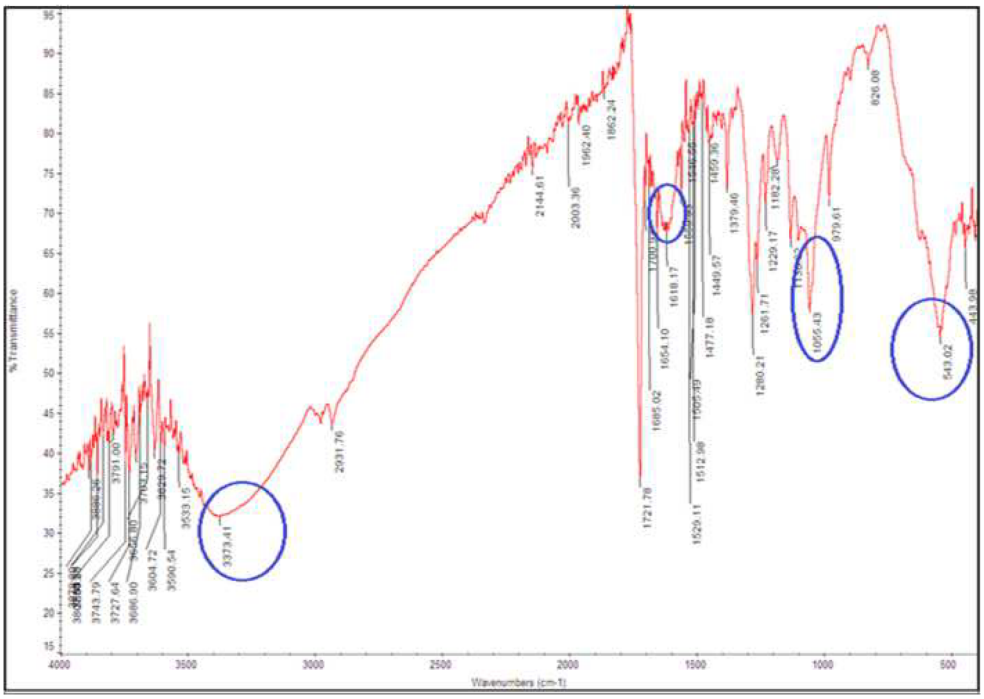

Fig. 4 FT-IR analyses of *Annona muricata* extract-loaded PHB-MNPs

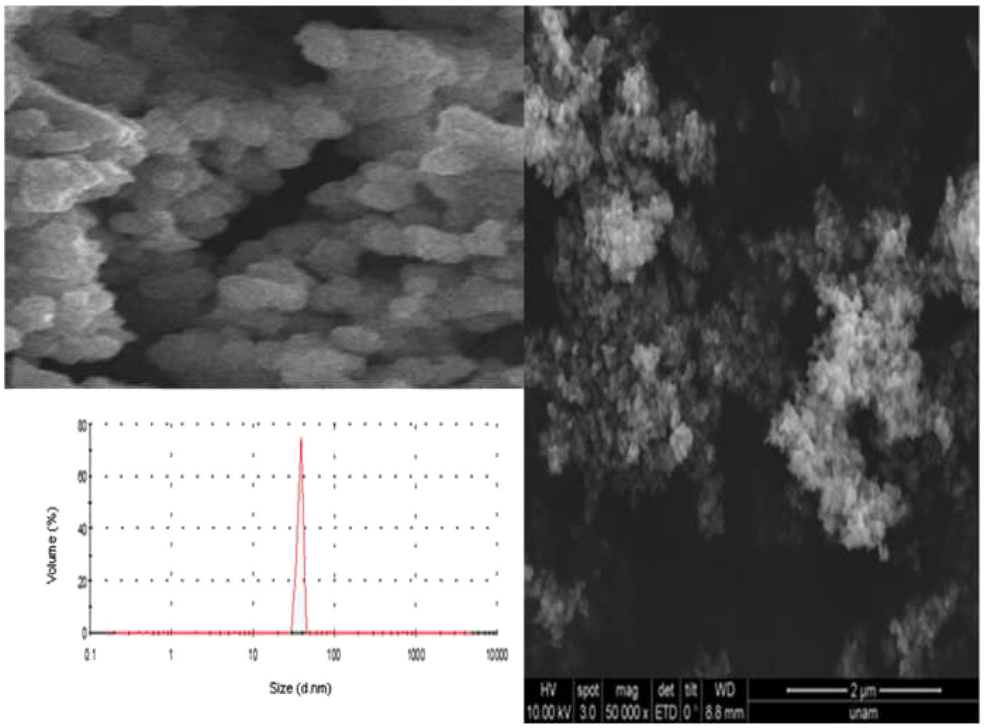

Fig. 5 SEM analyses of *Annona muricata* extract-loaded PHB-MNPs

serum, trypsin–EDTA, phosphate-buffered saline (PBS), and penicillin/streptomycin were purchased from Sigma-Aldrich (Chemie GmbH, Germany). The cell proliferation assay kit was supplied by Biotium 30007. HeLa and MDA-MB-231 cell lines were obtained from Erciyes University (Kayseri, Turkey).

Preparation of *A. muricata* Plant Leaf Extract

Commercially purchased *A. muricata* leaf extract was dissolved in 0.1% DMSO. Afterward, the supernatant was filtered off by centrifugation [20].

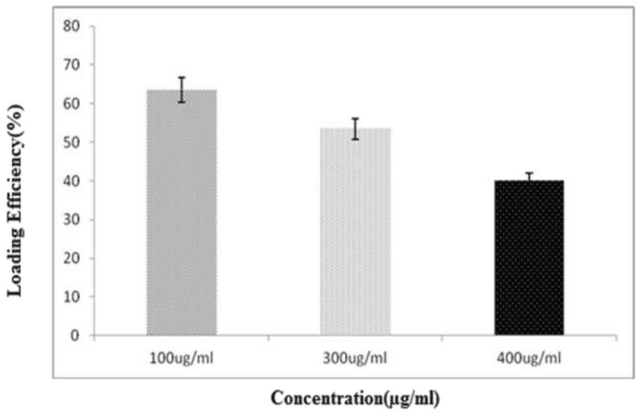

Fig. 6 Loading efficiencies of different concentrations of *Annona muricata* extract to PHB-MNPs

Synthesis and Characterization of PHB-Coated Magnetic Iron Oxide Nanoparticles (PHB-MNPs)

PHB-MNPs were in situ synthesized by the coprecipitation of Fe (II) and Fe (III) salts in the presence of PHB molecules with some modifications of Xiong et al. [21] and Yalcin et al. [6]. The characterization of PHB-MNPs was assessed by X-ray diffraction (XRD), Fourier-transform infrared spectroscopy (FTIR), thermal gravimetric analysis (TGA-FTIR), and vibrating sample magnetometry (VSM) analyses [6].

Extract Loading on PHB-Coated Magnetic Iron Oxide Nanoparticles

Loading studies of extract were carried out in PBS (pH 7.4), in different drug concentrations (100, 300, and 400 µg/ml). The mixture of buffer, extract, and PHB-MNPs was rotated for 24 h in a Falcon tube. After the rotation, extract-loaded PHB-MNPs were separated by magnetic separation, and the extract-loading efficiency was quantified by measuring the absorbance values at 286 nm by a UV spectrophotometer. The loading or binding of maximum extract-loaded concentration to the PHB-MNPs was confirmed by FTIR analysis.

Release and Stability of Extract on PHB-Coated Magnetic Iron Oxide Nanoparticles

Stabilities of extract-loaded PHB-MNPs were studied in PBS buffer (pH 7.4) at 37 °C up to 3 months. Extract stabilities

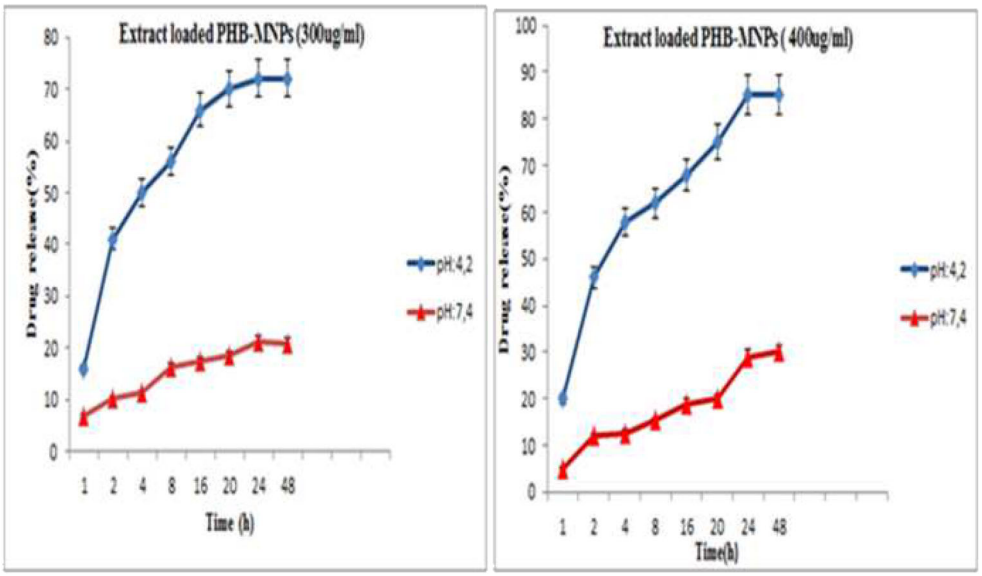

Fig. 7 Release of *Annona muricata* extract from PHB-MNPs

were measured as the absorbance values at 286 nm by a UV spectrophotometer. The release of extract (300 and 400 μg/ml) from PHB-MNPs was analyzed in acetate buffer with pH 4.2 and PBS buffer with pH 7.4 up to 48 h. The amount of released doxorubicin was determined by the decrease in the absorbance of the solution at 286 nm by a UV spectrophotometer.

Characterization of Extract-Loaded PHB-Coated Magnetic Iron Oxide Nanoparticles (PHB-MNPs)

The characterization of extract-loaded PHB-MNPs was assessed by FTIR spectroscopy, scanning electron microscopy (SEM), and dynamic light scattering (DLS) analyses.

Cellular Uptake

To determine the cellular internalization, extract-loaded PHB-MNPs were incubated for 24 h at 37 °C with HeLa and MDA-MB-231 cell lines in 12-well plates. Cells' photographs were taken by fluorescence microscopy after 5 h to determine their cellular internalization (BAB, Turkey).

Cytotoxicity of Extract-Loaded PHB-MNPs on HeLa and MDA-MB-231 Cell Lines

Cytotoxicity of PHB-MNPs, free extract, and extract-loaded PHB-MNPs on HeLa and MDA-MB-231 cell lines was determined by XTT Cell Proliferation Assay. According to the instructions of the manufacturer, XTT proliferation kit (Biotium 30007) was added after the cells were exposed to different concentrations of PHB-MNPs, free extract, and extract-loaded PHB-MNPs for 48–72 h. The cell viability of control groups was considered 100%. The amount of soluble product formazan dye was measured at 475 nm by a microplate reader (BIOTEK-ELX808 absorbance reader) and IC_{50} values were calculated from curves.

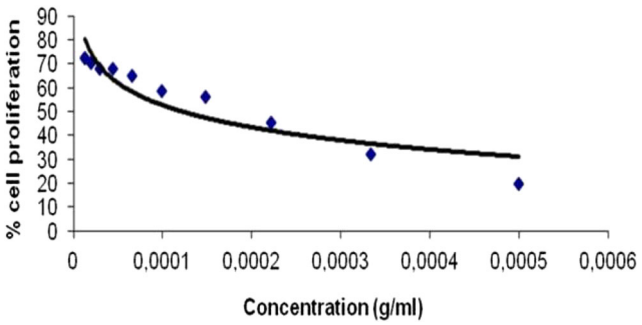

Fig. 8 Cytotoxic effect of *Annona muricata* extract on HeLa cells (IC_{50} = 180 μg/mL)

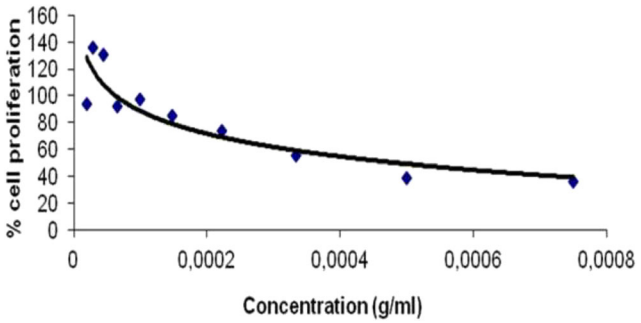

Fig. 9 Cytotoxic effect of *Annona muricata* extract on MDA-MB-231 cells (IC_{50} = 330 μg/mL)

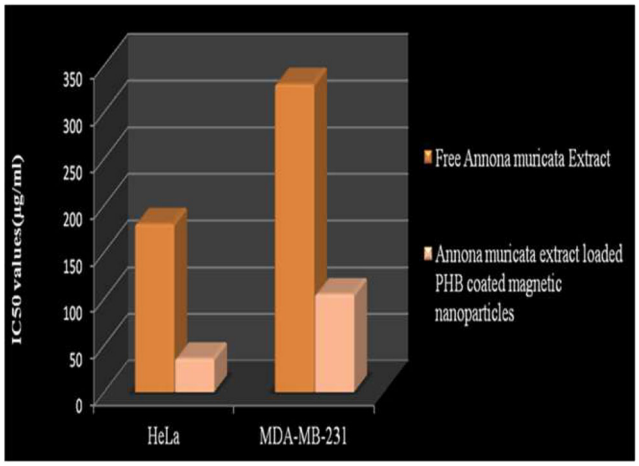

Fig. 10 Cytotoxic effect of *Annona muricata* extract-loaded PHB-MNPs on HeLa and MDA-MB-231 cells

Molecular Docking

The binding energy levels of isoquercetin, roseoside, and anonaine and isoquercetin–PHB-MNPs, roseoside–PHB-MNPs, and anonaine–PHB-MNPs with human Bcl-2, Bcl-w, Braf, Bcl-Xl, Bfl-1 proteins were calculated by using molecular docking method.

For ligand preparation, all the molecular structures of isoquercetin–PHB-MNPs, roseoside–PHB-MNPs, and anonaine–PHB-MNPs were sketched using GAUSSIAN09 [22]. The intended crystal protein structures were obtained from the protein data bank (www.rcsb.org) (Bcl-2 PDB ID, 4MAN; Bcl-w PDB ID, 2Y6W; Braf PDB ID, 5vam; Bcl-Xl PDB ID, 3IO8; Bfl-1 PDB ID, 5UUK). Molecular docking calculations were performed via Lamarckian Generic Algorithm [23] in Autodock Vina [24, 25]. All bound water molecules and ligands were removed from the proteins; non-polar hydrogen atoms were merged and the polar hydrogen atoms were added. The Molegro Molecular Viewer 2.5 (Molegro Molecular Viewer academic free software) and VMD (Visual Molecular Dynamic) [25] programs were used in the visualization of protein–ligand interaction [26].

Statistical Analysis

Data analyses were expressed as mean ± standard error of mean (SEM). Statistical analyses were performed with SPSS (10) software by using ANOVA, with $p < 0.05$ considered to represent statistical significance.

Results

In this work, we aimed to identify the most appropriate concentration, and stable and efficient magnetic drug delivery system for cancer therapy. The synthesis conditions of PHB-MNPs were optimized, and characterization of synthesized PHB-MNPs was performed by FTIR, TEM, TGA, and VSM analyses [6]. The FTIR spectrum was analyzed on the solid as KBr disc/pellets. This spectrum was recorded in the range of 4000–400 cm^{-1} at room temperature with Thermo Scientific Nicolet 6700 FT-IR instrument at Kırşehir Ahi Evran University, Central Research and Application Laboratory. In Figs. 1, 2, 3,

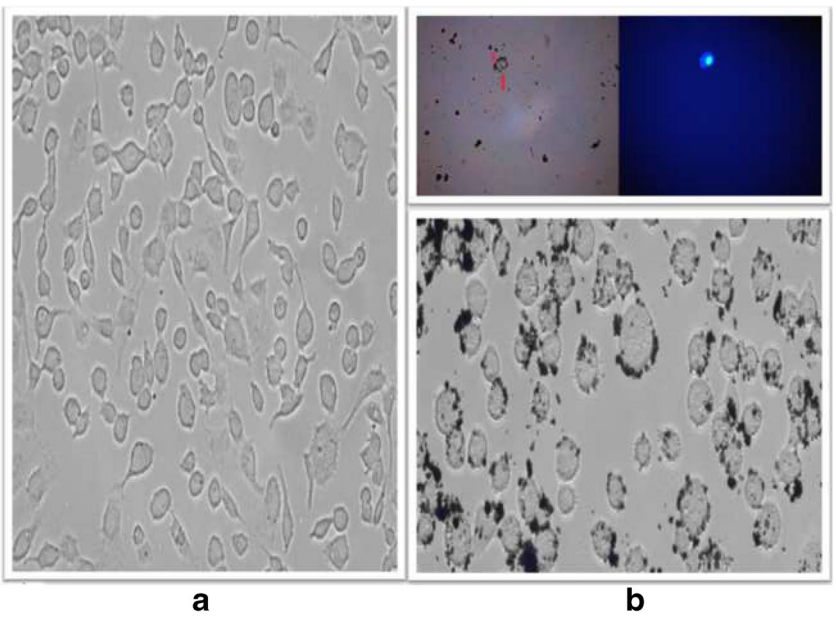

Fig. 11 Cellular internalization of *Annona muricata* extract-loaded PHB-MNPs by fluorescence microscopy and inverted microscopy (×20). (**a**) Control, (**b**) Treated cells

Table 1 Docking binding energy results of annonaine and annonaine–PHB nanoparticle molecule with proteins

Molecule	Protein	Binding energy (kcal/mol)	PDB ID
Anno	Bcl-2	− 8.6	4MAN
Anno	Bcl-w	− 9.0	2Y6W
Anno	Braf	− 9.7	5VAM
Anno	Bcl-Xl	− 8.5	3İO8
Anno	Bfl-1	− 7.9	5UUK
Anno-PHB nanoparticle	Bcl-2	− 12.0	4MAN
Anno-PHB nanoparticle	Bcl-w	− 12.5	2Y6W
Anno-PHB nanoparticle	Braf	− 13.4	5VAM
Anno-PHB nanoparticle	Bcl-Xl	− 13.2	3IO8
Anno-PHB nanoparticle	Bfl-1	− 13.0	5UUK

and 4, FTIR results showed the pure PHB, PHB-MNPs, pure *A. muricata* extract, and *A. muricata* extract-loaded PHB-MNPs, respectively. In Fig. 1, presence of iron oxide in PHB-MNPs (546.11 cm^{-1}). A strong peak of PHB at 1723.83 cm^{-1} indicates the stretching of C–O ester bond. The FTIR spectra of pure *A. muricata* extract and *A. muricata* extract-loaded PHB-MNPs are also shown in Figs. 3 and 4. The peaks at 1618.17, 1055.43, and 543.02 cm^{-1} indicated that *A. muricata* extract was loaded to PHB-MNPs.

Size and morphology of synthesized PHB-MNPs were observed by SEM (Fig. 5). On the bound size distribution graph, the MNP size was observed to be approximately 30–40 nm. *A. muricata* extract loading studies were performed in PBS buffer (pH 7.4) and the most efficient drug loading capacity increased up to 400 μg/ml on PHB-MNPs (Fig. 6). The most efficiently loaded extract concentrations (300 and 400 μg/ml) were selected, and release studies were analyzed in acetate buffer at pH 4.2 that mimics endosomal conditions; the release studies were continued up to 48 h. About 48% of drug released from 400 μg/ml extract-loaded nanoparticles in 2 h (Fig. 7).

The cytotoxic effect of extract and extract-loaded nanoparticles on HeLa and MDA-MB-231 cells was investigated by cell proliferation assay, and IC_{50} values were calculated (Figs. 8, 9, and 10). In this study, empty PHB-MNPs were found not to be significantly cytotoxic up to 500 μg/ml on different cancer cell lines [6] and healthy cells (MCF-10A) up to 1000 μg/ml. Therefore, PHB-MNPs have the ability to carry anti-cancer drugs safely [6].

The extract PHB-MNPs were about 2.7- and 3-fold more cytotoxic as compared with free extract on HeLa and MDA-MB-231 in vitro, respectively. The cellular internalization of extract-loaded nanoparticles was demonstrated by microscopy (Fig. 11).

Molecular docking studies have a critical role for molecular biology and drug discovery study. In this project, the efficient binding formation of anti-apoptotic protein–nanoparticle complexes was discovered with molecular docking analysis. Isoquercetin–PHB-MNPs, roseoside–PHB-MNPs, and anonaine–PHB-MNPs have been found to have higher

Table 2 Docking binding energy results of isoquercetin and isoquercetin–PHB nanoparticle molecule with proteins

Molecule	Protein	Binding energy (kcal/mol)	PDB ID
Isoquercetin	Bcl-2	− 9.9	4MAN
Isoquercetin	Bcl-w	− 10.9	2Y6W
Isoquercetin	Braf	− 9.8	5VAM
Isoquercetin	Bcl-Xl	− 10.6	3IO8
Isoquercetin	Bfl-1	− 8.3	5UUK
Isoquercetin–PHB nanoparticle	Bcl-2	− 15.8	4MAN
Isoquercetin–PHB nanoparticle	Bcl-w	− 17.9	2Y6W
Isoquercetin–PHB nanoparticle	Braf	− 16.2	5VAM
Isoquercetin–PHB nanoparticle	Bcl-Xl	− 16.5	3IO8
Isoquercetin–PHB nanoparticle	Bfl-1	− 13.9	5UUK

Table 3 Docking binding energy results of roseoside and roseoside–PHB nanoparticle molecule with proteins

Molecule	Protein	Binding energy (kcal/mol)	PDB ID
Roseoside	Bcl-2	− 7.7	**4MAN**
Roseoside	Bcl-w	− 9.5	2Y6W
Roseoside	Braf	− 9.2	5VAM
Roseoside	Bcl-Xl	− 8.9	3İO8
Roseoside	Bfl-1	− 7.6	5UUK
Roseoside–PHB nanoparticle	Bcl-2	− 13.5	4MAN
Roseoside–PHB nanoparticle	Bcl-w	− 19.0	2Y6W
Roseoside–PHB nanoparticle	Braf	− 15.9	5VAM
Roseoside–PHB nanoparticle	Bcl-Xl	− 15.3	3İO8
Roseoside–PHB nanoparticle	Bfl-1	− 14.4	5UUK

binding energies compared to free isoquercetin, roseoside, and anonaine. The docking study is based on the hypothesis that the isoquercetin–PHB-MNPs, roseoside–PHB-MNPs, and anonaine–PHB-MNPs are capable of interfering with the anti-apoptotic proteins and cause inhibition of their activity and cancer progression (Tables 1, 2, 3, and 4). The ligand–protein complex is shown in Figs. 12 and 13). Both in vitro cytotoxicity and molecular docking analyses revealed the increased toxicity of extract-loaded PHB-MNPs on MDA-MB-231 and HeLa cancer cell lines.

Discussion

A. muricata has been discovered as an abundant source of bioactive compounds in recent years, while the use of plants has acquired scientific and technological importance for drug development for millennia [27]. Recently, extract of *A. muricata* has shown antiproliferative effects against various cancer types such as colon, lung, and breast cancer cells by inhibiting mitochondrial complex I, which is related to oxidative phosphorylation and ATP synthesis [16, 28–32]. In this study, cells were treated to 500–1000 μg/ml of PHB-MNPs, and toxic effects were not observed on HeLa, MDA-MB-231, and MCF-10A cell lines. Combination of extract PHB-MNPs demonstrated excellent cytotoxic effect in breast cancer cell lines. Sabapati and Palei developed *A. muricata* fruit extract-loaded solid lipid nanoparticles (SLNs) and revealed its efficiently cytotoxic effect in an in vitro model [14].

Molecular docking studies were designed to analyze the protein–ligand interactions. In the present study, we analyzed anti-apoptotic Bcl-2, Bcl-w, Braf, Bcl-Xl, and Bfl-1 proteins with isoquercetin, roseoside, anonaine, and isoquercetin–PHB-MNP, roseoside–PHB-MNP, and anonaine–PHB-MNP ligands. The molecular docking results found a strong binding energy of isoquercetin–PHB-MNP, roseoside–PHB-MNP, and anonaine–PHB-MNP ligands with proteins when compared to isoquercetin, roseoside, and anonaine ligands. Antony and Vijayan found that the acetogenins, such as annomuricin A, annohexocin, muricatocin A, annomuricin-D-one, and muricatetrocin A/B, exhibited strong binding

Table 4 Docking binding energy results of doxorubicin (control) as inhibitor with proteins

Molecule	Protein	Binding energy (kcal/mol)	PDB ID
Doxorubicin	Bcl-2	− 9.0	4MAN
Doxorubicin	Bcl-w	− 9.0	2Y6W
Doxorubicin	Braf	− 9.7	5VAM
Doxorubicin	Bcl-Xl	− 9.7	3İO8
Doxorubicin	Bfl-1	− 8.6	5UUK

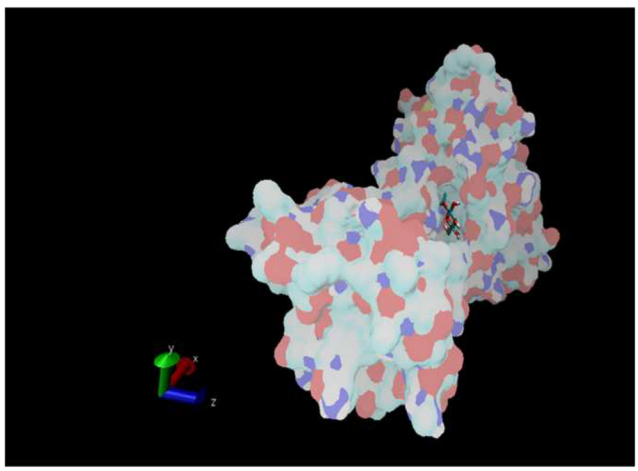

Fig. 12 The interaction of Bcl-w and roseoside molecule were visualized by VMD

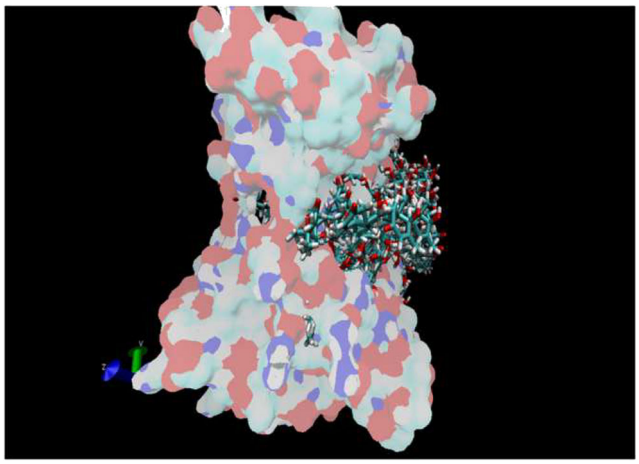

Fig. 13 The interaction of Bcl-w and roseoside–PHB nanoparticle were visualized by VMD

interactions with Bcl-Xl when compared to Bcl-2 and Mcl-1 [33]. Lannuzel et al. reported that the consumption of Annonaceae may contribute to the pathogenesis of atypical parkinsonism [34]. On this basis, we developed a low-dose extract-loaded nanoparticle system for targeted therapy. In this way, it is aimed to prevent the formation of different diseases while treating cancer.

Conclusion

In this study, extract-loaded nanoparticles were synthesized using a novel optimization approach and synthesized PHB-MNPs have shown a promising application in the pharmaceutical industries for cancer therapy. The free extract and extract-loaded PHB-MNPs were evaluated against cancer cell lines in vitro, looking at different concentrations and preparations of the plant extracts. Molecular docking studies were also used to support the cytotoxicity analyses. Further, this study suggests that the selected acetogenins can be further investigated and evaluated for cancer treatment in in vivo research and advanced computer analyses.

Acknowledgments This research was supported by Kirsehir Ahi Evran University Scientific Research Projects FEF.A4.17.018 (2018–2019).

Compliance with Ethical Standards

Conflict of Interest None declared.

Human and Animal Rights and Informed Consent This article does not contain any studies with human or animal subjects performed by any of the authors.

References

Papers of particular interest, published recently, have been highlighted as:
- • Of importance
- •• Of major importance

1. Erci F, Cakir-Koc R, Isildak I. Green synthesis of silver nanoparticles using Thymbra spicata L. var. spicata (Zahter) aqueous leaf extract and evaluation of their morphology dependent antibacterial and cytotoxic activity. Artif Cells Nanomed Biotechnol. 2018;46(sup1):150–8.
2. Palanisamy S, Wang YM. Superparamagnetic iron oxide nanoparticulate system: synthesis, targeting, drug delivery and therapy in cancer. Dalton Trans. 2019;48(26):9490–515.
3. Sanna V, Pala N, Sechi M. Targeted therapy using nanotechnology: focus on cancer. Int J Nanomedicine. 2014;9:467–83.
4. Yalcin S. Dextran-coated iron oxide nanoparticle for delivery of miR-29a to breast cancer cell line. Pharm Dev Technol. 2019;24(8):1032–7.
5. Arias LS, Pessan JP, Vieira APM, Lima TMT, Delbem ACB, Monteiro DR. Iron oxide nanoparticles for biomedical applications: a perspective on synthesis, drugs, antimicrobial activity, and toxicity. Antibiotics (Basel). 2018 ;7(2). pii: E46.
6. Yalcin S, Khodadust R, Unsoy G, Ceren Garip I, Didem Mumcuoglu Z, Gunduz U. Synthesis and characterization of polyhydroxybutyrate coated magnetic nanoparticles: toxicity analyses on different cell lines. Synthesis and Reactivity in Inorganic, Metal-Organic, and Nano-Metal Chemistry. 2015;45(5):700–8.
7. Vandamme P, Coenye T. Taxonomy of the genus Cupriavidus: a tale of lost and found. Int J Syst Evol Microbiol. 2004;54(Pt 6): 2285–9.
8. Bonartsev AP, Myshkina VL, Nikolaeva DA, Furina EK, Makhina TA, Livshits VA, et al. Biosynthesis, biodegradation, and application of poly (3-hydroxybutyrate) and its copolymers-natural polyesters produced by diazotrophic bacteria. Communicating Current Research and Educational Topics and Trends in Applied Microbiology. 2007;1:295–307.
9. Jendrossek D, Handrick R. Microbial degradation of polyhydroxyalkanoates. Annu Rev Microbiol. 2002;56:403–32.
10. Jacobo-Herrera N, Pérez-Plasencia C, Castro-Torres VA, Martínez-Vázquez M, González-Esquinca AR, Zentella-Dehesa A. Selective acetogenins and their potential as anticancer agents. Frontiers in Pharmacology. 2019:10.
11. Coria-Téllez AV, Montalvo-Gónzalez E, Yahia EM, Obledo-Vázquez EN. Annona muricata: a comprehensive review on its traditional medicinal uses, phytochemicals, pharmacological activities, mechanisms of action and toxicity. Arab J Chem. 2018;11(5): 662–91.
12. Gavamukulya Y, Wamunyokoli F, El-Shemy HA. Annona muricata: is the natural therapy to most disease conditions including cancer growing in our backyard? A systematic review of its research history and future prospects. Asian Pac J Trop Med. 2017;10(9):835–48.
13. Gavamukulya Y, El-Shemy HA, Meroka AM, Madivoli ES, Maina EN, Wamunyokoli F, et al. Advances in green nanobiotechnology: data for synthesis and characterization of silver nanoparticles from ethanolic extracts of fruits and leaves of Annona muricata. Data Brief. 2019;25:104194.
14. Sabapati M, Palei NN, AK CK, Molakpogu RB. Solid lipid nanoparticles of Annona muricata fruit extract: formulation, optimization and in vitro cytotoxicity studies. Drug Dev Ind Pharm. 2019;45(4):577–86.

15. Rupprecht JK, Hui YH, McLaughlin JL. Annonaceous acetogenins: a review. J Nat Prod. 1990;53(2):237–78.
16. McLaughlin JL. Paw paw and cancer: annonaceous acetogenins from discovery to commercial products. J Nat Prod. 2008;71:1311–21.
17. Degli Esposti M, Ghelli A, Ratta M, Cortes D, Estornell E. Natural substances (acetogenins) from the family Annonaceae are powerful inhibitors of mitochondrial NADH dehydrogenase (complex I). Biochem J. 1994;301(Pt 1):161–7.
18. Ribeiro AF, Santos JF, Mattos RR, Barros EGO, Nasciutti LE, Cabral LM, et al. Characterization and in vitro antitumor activity of polymeric nanoparticles loaded with Uncaria tomentosa extract. An Acad Bras Cienc. 2020;92(1):e20190336.
19. Piazzini V, Vasarri M, Degl'Innocenti D, Guastini A, Barletta E, Salvatici MC, et al. Comparison of chitosan nanoparticles and soluplus micelles to optimize the bioactivity of *Posidonia oceanica* extract on human neuroblastoma cell migration. Pharmaceutics. 2019;11(12):pii: E655.
20. Moghadamtousi SZ, Fadaeinasab M, Nikzad S, Mohan G, Ali HM, Kadir HA. Annona muricata (Annonaceae): a review of its traditional uses, isolated acetogenins and biological activities. Int J Mol Sci. 2015;16(7):15625–58.
21. Xiong YC, Yao YC, Zhan XY, Chen GQ. Application of polyhydroxyalkanoates nanoparticles as intracellular sustained drug-release vectors. J Biomater Sci Polym Ed. 2010;21(1):127–40.
22. Frisch MJ, Trucks GW, Schlegel HB, Scuseria GE, Robb MA, Cheeseman JR, … . Nakatsuji H. Gaussian09 Revision D. 01, Gaussian Inc. Wallingford CT. 2009. See also: URL: http://www.gaussian.com.
23. Morris GM, Goodsell DS, Halliday RS, Huey R, Hart WE, Belew RK, et al. Automated docking using a Lamarckian genetic algorithm and an empirical binding free energy function. J Comput Chem. 1998;19(14):1639–62.
24. Trott O, Olson AJ. AutoDock Vina: improving the speed and accuracy of docking with a new scoring function, efficient optimization, and multithreading. J Comput Chem. 2010 Jan 30;31(2):455–61.
25. Humphrey W, Dalke A, Schulten K. VMD: visual molecular dynamics. J Mol Graph. 1996;14(1):33–8 **27-8**.
26. Thomsen R, Christensen MH. MolDock: a new technique for high-accuracy molecular docking. J Med Chem. 2006;49(11):3315–21.
27. Badrie N, Schauss AG. Soursop (*Annona muricata* L.): composition, nutritional value, medicinal uses, and toxicology in bioactive foods in promoting health. Academic Press. 2010:621–43.
28. Robles JF, Muñoz K, Rivera N, Suarez E. Anti-proliferative properties of methanolic extracts of Annona muricata in colon, lung and skin cancer cell lines. FASEB J. 2017;31:807–5.
29. Kim GS, Zeng L, Alali F, Rogers LL, Wu FE, McLaughlin JL, et al. Two new mono-tetrahydrofuran ring acetogenins, annomuricin E and muricapentocin, from the leaves of Annona muricata. J Nat Prod. 1998;61(4):432–6.
30. Eggadi V, Gundamedi S, Sheshagiri SBB, Revoori SK, Jupally VR, Kulandaivelu U. Evaluation of anticancer activity of Annona muricata in 1, 2-dimethyl hydrazine induced colon cancer. World Appl Sci J. 2014;32:444–50.
31. Deep G, Kumar R, Jain AK, Dhar D, Panigrahi GK, Hussain A, et al. Graviola inhibits hypoxia-induced NADPH oxidase activity in prostate cancer cells reducing their proliferation and clonogenicity. Sci Rep. 2016;6:23135.
32. Rady I, Bloch MB, Chamcheu RN, Banang Mbeumi S, Anwar MR, Mohamed H, et al. Anticancer properties of graviola (Annona muricata): a comprehensive mechanistic review. Oxidative Med Cell Longev. 2018;2018:1826170.
33. Antony P, Vijayan R. Acetogenins from Annona muricata as potential inhibitors of antiapoptotic proteins: a molecular modeling study. Drug Des Devel Ther. 2016;10:1399–410.
34. Lannuzel A, Höglinger GU, Champy P, Michel PP, Hirsch EC, Ruberg M. Is atypical parkinsonism in the Caribbean caused by the consumption of Annonacae? J Neural Transm Suppl. 2006;70:153–7.